

DETECTION OF LARGE FARADAY ROTATION IN THE INNER 2 KILOPARSECS OF M87

FRAZER N. OWEN¹National Radio Astronomy Observatory²

JEAN A. EILEK

Department of Physics and Astrophysics Research Center, New Mexico Tech

AND

WILLIAM C. KEEL¹

Department of Physics and Astronomy, University of Alabama

Received 1989 August 28; accepted 1990 April 17

ABSTRACT

VLA polarization maps of M87 at four frequencies between 4.635 and 4.935 GHz reveal large Faraday rotation measures in the direction of the 2 kpc radio lobes. Over most of the source the typical rotation measure is 1000 rad m^{-2} but values as high as 8000 rad m^{-2} are found in small regions. Most of the source has fractional polarization in excess of 10%. This fact coupled with the high rotation measures suggests that the rotation is taking place in a Faraday screen in front of the radio-emitting plasma rather than mixed with it. The observed scale sizes coupled with the X-ray density profile suggest that most of the rotation is taking place close to the scale size of the lobes. Over most of the source the rotation measures are smooth on scales of 500 pc to 1 kpc and the values are mostly positive, requiring a large ordered field component. Based on the radio structure of the lobes we estimate a magnitude of $\sim 40 \mu\text{G}$ for this component of the B field. The pressure corresponding to this field strength is interestingly close to the thermal pressure estimated from X-ray observations. Emission-line limits for the region of highest rotation measure show that this particular structure is either magnetically supported or confined, or must be overpressured and transient. The smallest rotation measures we see are in the direction of the jet. This suggests either that the jet probably lies mostly in front of the Faraday screen. We suggest that the overall pattern is most consistent with the Faraday screen lying in a moderately thick boundary layer enveloping the 2 kpc radio lobes.

Subject headings: galaxies: individual (M87) — galaxies: interstellar matter — galaxies: jets — polarization — radio sources: galaxies

I. INTRODUCTION

M87 has been a target of intense study at a variety of wavelengths since the connection of the strong radio source, Virgo A, with the Virgo cluster central galaxy and its strange jet by Baade and Minkowski (1954). Even though it is well known that the radio jet and the 2 kpc radio lobes are due to synchrotron emission, the Faraday rotation from that structure has never been studied with enough spatial and frequency resolution to pin down the properties of the source.

Since the discovery of the complex distribution of large Faraday rotation over the lobes of Cygnus A (Dreher, Carilli, and Perley 1987), we thought it would be interesting to study another object in a cooling core. Therefore, as part of a study of the structure of the radio lobes, we mapped the polarization structure of the lobes at four frequencies near 5 GHz with the VLA array. The results, which were quite surprising to us, are reported in this paper.

II. OBSERVATIONS AND REDUCTIONS

The observations reported in this paper were made for 10 hr on 1986 April 25 in the VLA A array at 6 cm. Observations

were made in four 50 MHz bands, centered at 4.635, 4.735, 4.835, and 4.935 GHz. 3C 286 was used as the polarization position angle calibrator for each band. 1252+119 was the secondary calibrator used to calibrate the instrumental polarization. After standard calibration, the data were self-calibrated and further processed as discussed by Hines, Owen, and Eilek (1989, hereafter HOE). After this processing the Q and U maps were made in the standard way using the AIPS programs UVMAP and APCLN. The total polarization, position angle, and error images were then calculated using COMB and taking into account the noise biases correctly using the POLC option. The position-angle maps and errors were then analyzed using RM to obtain an image of the rotation measures and their associated errors. Several points, including the largest rotation measures were then checked graphically to verify that the program was producing meaningful results. All the checked points showed that the four observed position angles fit λ^2 laws very well, except for a few of the highest points in the high rotation filament which will be discussed below. This result plus the continuity of the resulting rotation measure map gives us great confidence in the results.

III. RESULTS

Figure 1 (Plate 8) and Figure 2 present the distribution of rotation measure across the entire region of the inner lobes of M87. We find that the rotation measure is quite large and positive across most of the source: $\text{RM} \sim 1000\text{--}2000 \text{ rad m}^{-2}$ is typical.

¹ Visiting Astronomer at NOAO, operated by the Association of Universities for Research in Astronomy, Inc., under contract with the National Science Foundation.

² The National Radio Astronomy Observatory is operated by Associated Universities, Inc., under cooperative agreement with the National Science Foundation.

PLATE 8

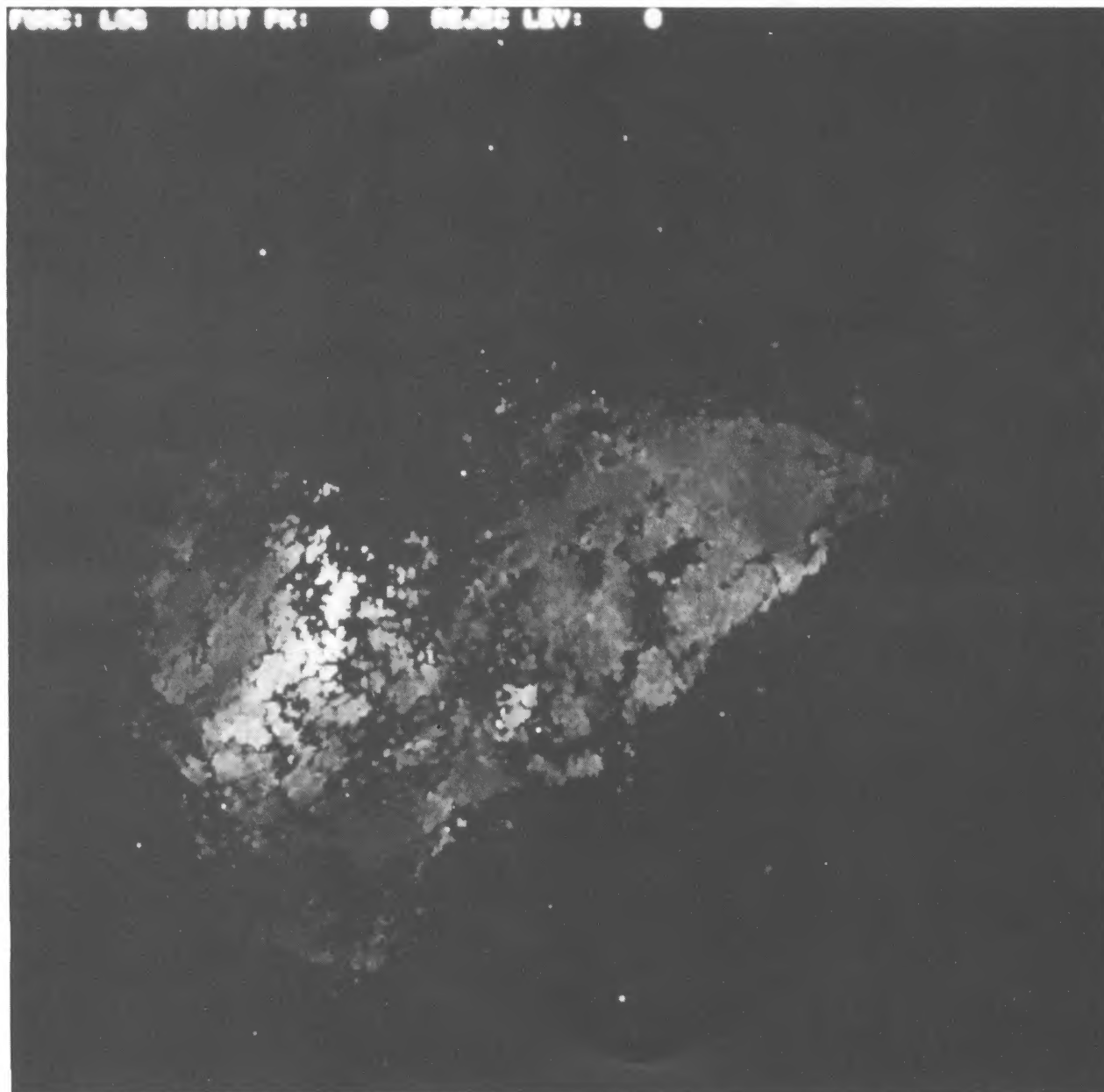


FIG. 1.—Gray scale of the rotation measure map of M87. The brightest areas show rotation measure $\sim 6000\text{--}8000 \text{ rad m}^{-2}$; the typical rotation measure for the western lobe, away from the jet, is $\sim 750\text{--}1000 \text{ rad m}^{-2}$. The inner jet has $\text{RM} \sim 200 \text{ rad m}^{-2}$.

OWEN, EILEK, AND KEEL (*see* 362, 449)

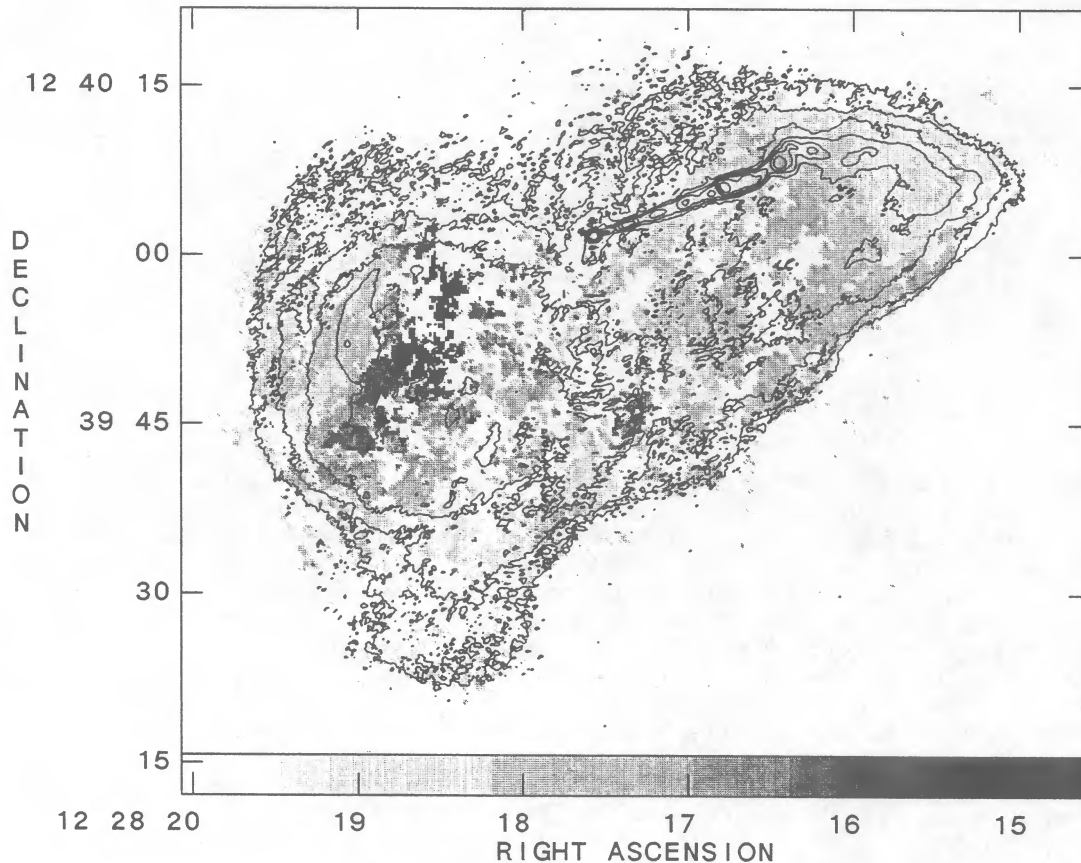


FIG. 2.—Gray scale of the total rotation measure field. Contour lines of the 6 cm total intensity map are shown, at levels $-1, 1, 2, 4, 8, 16, 32, 64, 128, 256,$ and 512 mJy beam^{-1} .

We see several striking features in these data. First, the rotation measure is positive over most of the source. The only significant areas with negative rotation measure are at the western end of the jet, where the jet appears to bend and twist entering the lobe; and a couple of areas on the outer edges of the eastern lobe. The magnitudes of these negative rotation measures about -1000 rad m^{-2} . Second, the jet can be clearly picked out in Figures 1 and 2 as an area of low rotation measure. We show the jet area in more detail in Figures 3 and 4. Except for high values ($\sim 2000 \text{ rad m}^{-2}$) just outside the core, the rotation measure along the jet less than $\sim 200 \text{ rad m}^{-2}$ for the first $\sim 15''$ (1.2 kpc). At this point an apparent filament of higher rotation measure ($\sim 750 \text{ rad m}^{-2}$) crosses the jet. This filament appears to connect to the area of comparable rotation measure just south of the jet. This occurs at feature C in the jet (see Owen, Hardee, and Cornwell 1989; OHC), just beyond the first wiggle in the jet; beyond this point, the jet bends and twists and appears to enter or blend into the lobe. Third, the lobes display a smooth, positive rotation measure, which increases from $\sim 750 \text{ rad m}^{-2}$ in the western lobe to $\sim 2000 \text{ rad m}^{-2}$ in the eastern lobe. Finally, the eastern lobe contains a small patch of much higher rotation measure; we show this area in detail in Figure 5. This high-RM filament has dimensions $\sim 1''$ by $\sim 10''$ ($\lesssim 80$ by $\sim 800 \text{ pc}$; the transverse scale may not be resolved). The typical rotation measure $\sim 6000 \text{ rad m}^{-2}$ along this filament, with the highest values reaching $\sim 8500 \text{ rad m}^{-2}$. This feature does not correspond to any of the bright filaments seen in the total intensity image of HOE.

IV. DISCUSSION

a) Where is Rotation Occurring?

Before we discuss the results in detail, we should ask where along the line of sight it is reasonable for the Faraday rotation to arise. Since the rotation follows a λ -squared law over as much as 720 degrees of rotation within the frequency interval 4.635–4.935 GHz without depolarizing the source, the rotating region must be in the foreground and not mixed with the emitting region (Laing 1986). The galactic contribution at this high galactic latitude is on the order of 10 rad m^{-2} . Also M84, another galaxy in the Virgo cluster shows much smaller rotation measures (Laing and Bridle 1987). Thus it seems likely that the rotation is isolated to the general region of M87.

Models of the X-ray emitting gas allow us to put further limits on what is expected. If we approximate the gas pressure and density distributions in M87 as power laws, i.e., $p \propto r^{-x}$ and $n \propto r^{-y}$, we find for the models of White and Sarazin (1988) $x \sim y \sim 0.5\text{--}1.0$ for $r_{\min} \lesssim r \lesssim 20\text{--}30 \text{ kpc}$ and $x \sim y \sim 1.0\text{--}1.5$ at larger distances. These models have $r_{\min} \sim 1 \text{ kpc}$, limited by the resolution of the HRI and the internal consistency of the models. Silk *et al.* (1986) point out that this pressure and density behavior is in agreement with the general trends of cooling-flow models, and that the density is especially robust in the face of various assumptions that go into the models.

Cluster scale magnetic fields have not been studied as thoroughly as the gas distribution, but we believe the same patterns will be followed, i.e., $B \propto r^{-z}$ where $z \sim 1\text{--}2$. We note three

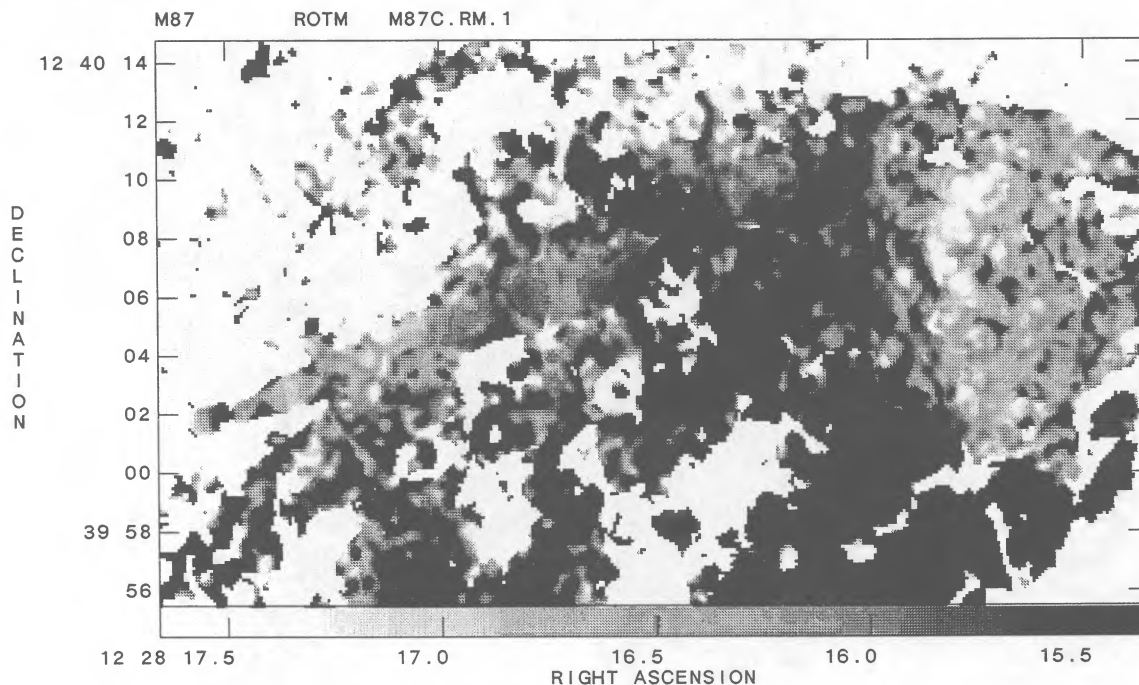


FIG. 3.—Rotation measure of the region around the jet of M87. Values above 350 rad m^{-2} are black.

arguments. First, the energy density of the cluster field is unlikely to exceed the thermal gas density (since the field must ultimately be bound by the gravitational potential of the cluster). This would suggest $B \lesssim B_{\text{max}} \sim (8\pi p)^{1/2} \propto r^{-x/2}$. Second, Soker and Sarazin (1989) have suggested a model in which cooling inflow and local reconnection result in a mostly radial magnetic field, which obeys $B \propto r^{-2}$, for $8 \lesssim r \lesssim 100$ kpc and an isotropic field, $B \propto p^{1/2}$ for $r < 8$ kpc. Finally, Eilek (1989) has noted that the dynamo equation in a turbulent ICM can be solved by fields which obey $B_r, B_\theta \propto r^{-2}$ and $B_\phi \propto r^{-1}$ for $r \gtrsim r_{\text{min}}$. In these models, r_{min} is set by the scale size of galaxy-driven turbulence: $r_{\text{min}} \sim 10\text{--}20$ kpc.

Thus, outside of some r_{min} , we expect the product nB to fall off as $r^{-1.75}$ to $r^{-3.5}$. Therefore we expect most of the rotation to occur inside of this r_{min} , which is between a few and ~ 20

kpc. Based on this argument, we will focus most of our attention on scales close to the radio source scale.

The patterns of rotation across the source also suggest a generally small scale for most of the rotation. From Figure 1, one can see resolved patches of rotation with scale size up to ~ 1 kpc, suggesting that regions of roughly this scale size produce most of the rotation.

b) Rotation in Direction of Jet

In contrast to the fairly high rotation measures seen over most of the lobes, relatively small rotation is seen in most directions along the jet. In Figure 3 we show a gray-scale plot of the rotation in the direction of the jet scaled so that rotations above 350 rad m^{-2} are black. In Figure 4 we show a plot of the value of the rotation along the center of the jet. The most striking thing is the relatively low value of rotation along the jet. Over most of the jet the absolute value of the rotation is less than 300 rad m^{-2} . Only two regions exceed this range, and they appear to be associated with gas very near the nucleus and with a larger pattern in the western lobe, respectively.

Since we believe the rotation is caused by a foreground screen, the relatively small rotation in the direction of the jet is rather surprising and must be giving us important clues to the three-dimensional structure of the region. If the foreground screen were unconnected and far in front of the source, one would expect the jet to be just as likely to be covered by the screen as the lobe. Also since the jet extends all the way into the nucleus, one might expect it would have a higher probability of being behind a rotating cloud. Instead the inner part of the jet, except for one point, shows the lowest rotation measures found in the source. Thus it seems that the jet must either lie in front or to one side of the high rotation measure region. However, at feature C, just beyond the region where the first wiggle occurs in the jet, it appears to pass behind a high rotation measure region. After this point the jet appears to bend and mix with the diffuse continuum emission from the radio lobe.

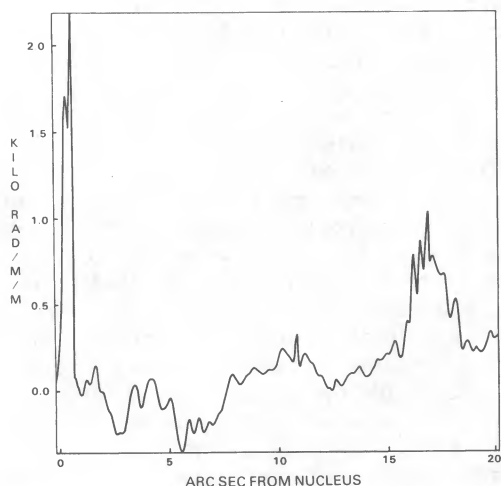


FIG. 4.—Rotation measure along the jet of M87. The data are plotted from the nucleus past knot C.

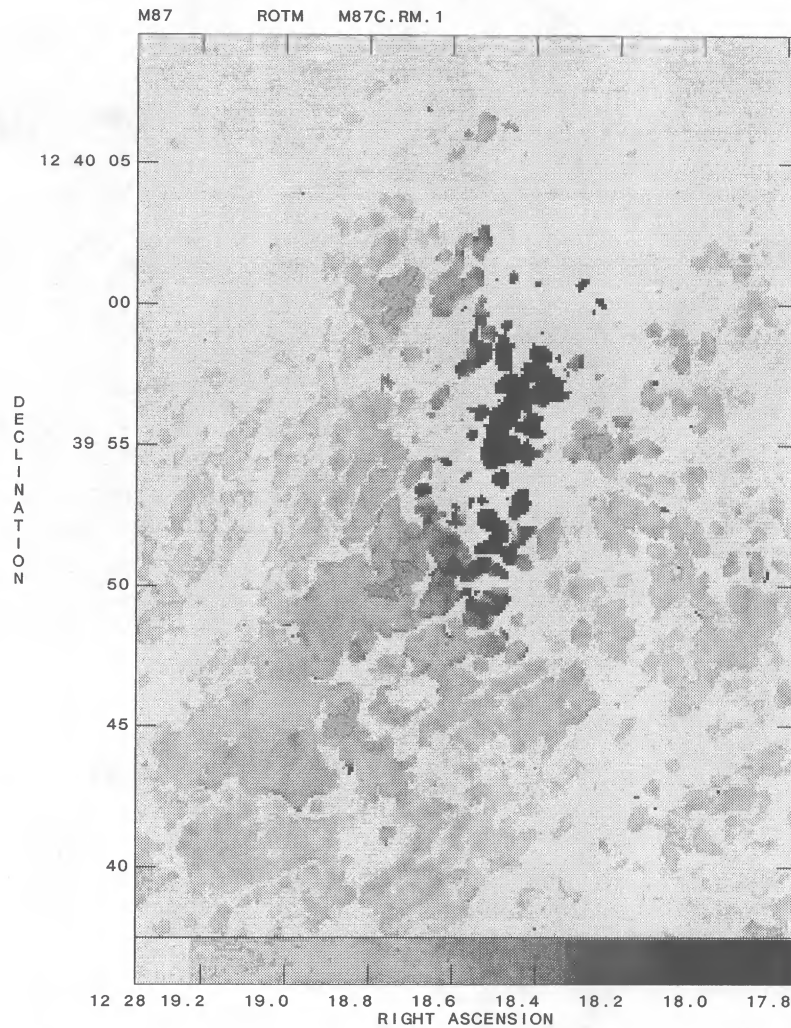


FIG. 5.—Rotation measure of the region around the high-RM patch in the east lobe

The simplest explanation of this pattern is that the foreground screen is associated with the general region of the 2 kpc lobes. As can be seen on any radio image of the lobes (e.g., HOE), the 2 kpc radio structure is primarily south of the center of the galaxy. If it is also bent back behind the plane of the sky as we see it, then most of the lobe structure would be behind the jet. The jet probably is near the plane of the sky but pointed slightly toward us and bends back toward the sky plane near knot C and gradually diffuses into the western lobe. This geometry is consistent with the independent deductions by OHC.

c) General Rotation Measure of Inner Lobes

The rotation measure over the inner lobes is, in general, smoothly distributed and positive; it increases from ~ 750 rad m^{-2} on the western lobe to ~ 2000 rad m^{-2} in the eastern lobe. This requires the magnetic field to have an ordered component along the line of sight, with the same sign across most of the lobes. We estimate this field by recalling the expression for rotation measure,

$$RM \simeq 800 \int nB \cdot dl \simeq 800n \langle B_{\parallel} \rangle L \text{ rad m}^{-2}.$$

Here, the magnetic field is measured in μG , the length L in kpc, and the number density in cm^{-3} . In the second expression we have substituted the mean number density along the line of sight, and the net path length L ; this means that the average magnetic field along the line of sight is measured: $\langle B_{\parallel} \rangle$.

For this general rotation measure distribution across the source, it seems reasonable to use the number density inferred from models of the X-ray emitting gas (most recently, White and Sarazin, 1988). OHC have scaled these models to 17 Mpc (see also HOE) and estimate $n \sim 0.15 \text{ cm}^{-3}$, $T \sim 2 \times 10^7 \text{ K}$ for the inner 1–2 kpc. We believe the most likely location for this general rotation measure is a moderately thick shell surrounding the radio lobes. As discussed above, the exceptionally low rotation measures for the inner jet require the jet either to lie in front of the material which rotates the lobes, or to lie in a central ~ 1 kpc “hole” in the rotation measure. In addition, the scale of variations in rotation measure across the inner lobes ~ 1 kpc. Finally, the typical RM in the eastern lobe is ~ 3 times that in the western lobe, which is the approximate ratio of sizes of the lobes as projected on the sky.

One possibility is that diffuse regions seen on the images discussed by HOE surrounding the brightest and most polarized part of the lobes can be identified with the Faraday

screen. Unfortunately, the final reproductions of the images in HOE do not show these regions clearly; but on the original images one can see a diffuse halo of emission surrounding the highly filamented parts of the source. These halo regions have projected thicknesses of ~ 1 kpc and 0.3 kpc on average surrounding the eastern and western lobes, respectively. Assuming these regions contain the Faraday screen, we estimate $\langle B_{\parallel} \rangle \sim 25 \mu\text{G}$ surrounding both lobes. If the field is well ordered but not totally in the line of sight, the true field value will be increased by $\sim 3^{1/2}$, to $\sim 40 \mu\text{G}$. This value is interestingly close to the value derived from a minimum-pressure analysis on the "background" in the radio lobes (the diffuse emission which is not obviously part of the bright filaments). HOE find $B_{\text{min } p} \sim 22 \mu\text{G}$ for this background. One is tempted to speculate from this that the magnetic field within the radio source has somehow mixed with the external thermal plasma, in a surface layer between the radio luminous plasma and the interstellar medium. One could even speculate further that this is the low surface brightness layer seen by HOE.

Another interesting point is that this magnetic field value, $40 \mu\text{G}$, is not that far from being dynamically important. The field value for which magnetic energy density equals the thermal gas pressure in this region is $B = (8\pi p)^{1/2} \sim 100 \mu\text{G}$. Given the uncertainty in the geometry, it seems quite possible that the actual field could be dynamically important.

d) High Rotation Measure Filament

The highest rotation measures we detected were in the eastern lobe along an arc $\sim 10''$ in projected length. In Figure 5 we show a blowup of the gray scale. Values of the rotation measure range from ~ 4000 to 8500 rad m^{-2} in this region. No obvious feature in the continuum map corresponds to this feature. The regions of highest rotation measure seem to be unresolved perpendicular to the filament with a size certainly less than $1''$.

The points on the rotation measure map with values above $\sim 6000 \text{ rad m}^{-2}$ show a small deviation from a λ^2 law ($\sim 20^\circ$) in excess of the noise. In most cases these values are consistent with much larger values of the rotation measure. However, these slightly discrepant values are consistent with a combination of sharp gradients across the feature and shifts in effective wavelength due to the large (50 MHz) bandwidth we used. Higher frequency maps will be necessary in order to completely resolve the situation by improving the resolution and reducing the bandwidth effects.

In order to determine the magnetic field in this high-RM features, we investigated limits on the gas density in that region. In addition to the gas pressure estimates from the (scaled) White and Sarazin models, we used limits on the X-ray and line emission fluxes. For the X-ray limits, John Biretta (1988, private communication) has kindly supplied us with the excess X-ray emission (above the general galactic halo) measured by the *Einstein* HRI detector in a $10''$ aperture centered on the east lobe of M87. The emission is modeled to be thermal; if it is assumed all to come from the filament, we derive upper limits to the filament emissivity.

To get emission line limits, we obtained a long slit spectrum aligned with the filament using the Gold spectrograph with the TI CCD in a 2 hr exposure on the 2.1 m telescope at NOAO. For our limits we have analyzed a $2'' \times 4''$ aperture coincident with the brightest part of the RM filament. The resolution was optimized for line widths approximately equal to the stellar velocity dispersion, and the repeatability of the offsetting was

$1''$. The data reduction and determination of detection limits were done as discussed in Owen, O'Dea, and Keel (1989). No line emission was detected at H α (at a level of 20% of the stellar absorption) giving a flux limit of $3.7 \times 10^{-17} \text{ ergs cm}^{-2} \text{ arcsec}^{-2}$. Nor was any emission seen in the [Fe x] $\lambda 6374$ and [Fe xiv] $\lambda 5303$ lines (for an upper limit of $6 \times 10^{-18} \text{ ergs cm}^{-2} \text{ arcsec}^{-2}$ in each line). These data give us limits on the volume emissivity in each line.

We show these limits in Figure 6. We convert the emissivity limits to temperature-dependent density limits using the X-ray emissivity from Zombeck (1980), the H α emissivity from Ferland (1980), and the Fe line emissivities from Nussbaumer and Osterbrock (1970). We assumed the filament is a cylinder, of diameter $1''$ (80 pc), lying in the plane of the sky. We also show in Figure 6 the region of density and temperature values which are consistent with the filament being in pressure balance with its surroundings, using the range of pressures estimated from the scaled White and Sarazin models. From Figure 6 we can account for the high RM values in two ways. One possibility is that the filament is cool ($T \lesssim 10^6 \text{ K}$) and in pressure balance with the X-ray gas, with all of the internal pressure due to the magnetic field: $\langle B_{\parallel} \rangle \sim 100 \mu\text{G}$ is needed. Alternatively, the field can be overpressured. In this case, it can have $T \gtrsim 10^6 \text{ K}$ and $1 \text{ cm}^{-3} \lesssim n \lesssim 10 \text{ cm}^{-3}$, in which case its internal gas pressure exceeds that of the surroundings. Or, it can have $n \lesssim 1 \text{ cm}^{-3}$, in which case its magnetic pressure must be greater than the surrounding gas pressure. Thus, if it is overpressured, it may be a magnetically confined structure, or it may be a transient feature. If the latter, it will dissipate in $\sim 80 \text{ pc}/(v_A^2 + c_s^2)^{1/2} \sim 4 \times 10^5 \text{ yr}$ (noting the sound speed

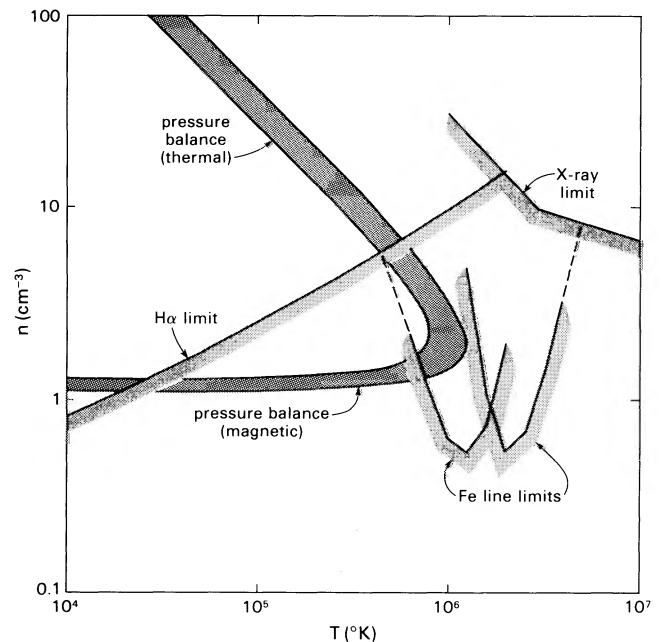


FIG. 6.—Density limits for the high-RM filament in the east lobe. The shaded band shows n and T values consistent with the pressure of the scaled White and Sarazin (1988) model (see text) in the region, $p \sim 3.7\text{--}5.0 \times 10^{-10} \text{ dyn cm}^{-2}$, and also consistent with the observed RM $\sim 800 \text{ rad m}^{-2}$ (but with no projection factor assumed for the magnetic field). The solid lines are upper limits on the density derived from observed H α , Fe line and X-ray emissivity limits. The dotted lines are extrapolations of the Fe line limits, outside of the temperature ranges calculated by Nussbaumer and Osterbrock (1970). The filament was assumed to be cylindrical, $1''$ (80 pc) in diameter, and to lie in the plane of the sky.

$c_s \gtrsim 200 \text{ km s}^{-1}$, and the Alfvén speed $v_A \gtrsim 20 \text{ km s}^{-1}$ with these limits).

The need for high field strengths in the feature can be reduced if its depth along the line of sight is greater than 80 pc. We applied the emissivity limits to the extreme case of a thin sheet, 800 pc deep and containing the line of sight. This formally allows a sheet in pressure balance, with $n \lesssim 1 \text{ cm}^{-3}$, $T \gtrsim 3 \times 10^6 \text{ K}$ and $B^2 < 8\pi p$. Such a feature will also be transient, however, since this temperature is probably thermally unstable; higher temperatures and lower densities require higher magnetic fields, which become dynamically important. Dropping the requirement of pressure balance (for instance in a shock) allows the observational constraints to be met, but again gives a short-lived situation. Thus, we again conclude the feature is either magnetically supported or transient.

V. CONCLUSIONS

The high Faraday rotation measures seen in the inner region of M87 suggest a complex region in which the magnetic field plays an important role.

1. The large patches of coherent, positive rotation distributed over the source suggest an ordered field on the scale of 1 kpc on the order of $40 \mu\text{G}$. If small-scale field reversals occur the local value of the field could be much larger. This field is probably dynamically important in the core region.

2. The low values of rotation in the direction of the jet suggest that the screen is associated with the regions of the lobes which are bent away from the plane of the sky, that the rotation is relatively small in the inner kpc, and that the jet thus sits in front of the high-rotation region.

3. The region of highest Faraday rotation is a filament with rotations ranging from 4000 to 8500 rad m^{-2} . Emission-line limits on the density show either that magnetic pressure supports this structure or that it is strongly overpressured and transient.

We are grateful to John Biretta for analyzing the *Einstein* data for the east lobe of the source and supplying us with easy-to-interpret numbers.

REFERENCES

- Baade, W., and Minkowski, R. 1954, *Ap. J.*, **119**, 221.
 Dreher, J. W., Carilli, C. L., and Perley, R. A. 1987, *Ap. J.*, **316**, 611.
 Eilek, J. A. 1989, in *Proc. STScI Workshop, Cluster of Galaxies*, ed. M. J. Fichett and W. R. Oegerle (NASA-STScI), p. 59.
 Ferland, G. 1980, *Pub. A.S.P.*, **92**, 596.
 Hines, D. C., Owen, F. N., and Eilek, J. A. 1989, *Ap. J.*, **347**, 713 (HOE).
 Laing, R. A. 1986, in *Physics of Energy Transport in Extragalactic Radio Sources*, ed. A. H. Bridle and J. A. Eilek (Green Bank: NRAO), p. 90.
 Laing, R. A., and Bridle, A. H. 1987, *M.N.R.A.S.*, **228**, 557.
 Nussbaumer, H., and Osterbrock, D. E. 1970, *Ap. J.*, **161**, 811.
 Owen, F. N., Hardee, P. E., and Cornwell, T. C., 1989, *Ap. J.*, **340**, 698 (OHC).
 Owen, F. N., O'Dea, C. P., and Keel, W. C. 1989, *Ap. J.*, **352**, 44.
 Silk, J., Djorgovski, S., Wyse, R. F. G., and Bruzual, G., 1986, *Ap. J.*, **307**, 415.
 Soker, N., and Sarazin, C. L. 1989, *Ap. J.*, **348**, 73.
 White, R. E., III, and Sarazin, C. L. 1988, *Ap. J.*, **335**, 688.
 Zombeck, M. V. 1980, *High Energy Astrophysics Handbook*, SAO Spec. Rept. 386.

JEAN A. EILEK: Department of Physics, New Mexico Tech, Socorro, MN 87801

WILLIAM C. KEEL: Department of Physics and Astronomy, University of Alabama, P.O. Box 870234, Tuscaloosa, AL 35487

FRAZER N. OWEN: NRAO, P.O. Box O, Socorro, NM 87801